Contents lists available at ScienceDirect

Journal of Orthopaedic Translation

journal homepage: www.journals.elsevier.com/journal-of-orthopaedic-translation

Original Article

Distinctive roles of tumor necrosis factor receptor type 1 and type 2 in a mouse disc degeneration model

Shanzheng Wang [a,1], Guodong Sun [b,c,1], Pan Fan [a], Lei Huang [d], Yaofei Chen [d], Changhong Chen [d,*]

[a] Department of Orthopedics, Affiliated Zhongda Hospital of Southeast University, Nanjing, Jiangsu, 210009, PR China
[b] Department of Orthopedics, First Affiliated Hospital, Jinan University, Guangzhou, 510632, PR China
[c] Clinical Biomechanics and Biomimetic Materials Research Center, Guangdong-Hong Kong-Macao Greater Bay Area, Jinan University, Guangzhou, 510632, PR China
[d] Department of Orthopedics, Jiangyin Hospital Affiliated to Nanjing University of Chinese Medicine, Wuxi City, Jiangsu, 214400, PR China

ARTICLE INFO

ABSTRACT

Background: Elevated tumor necrosis factor alpha (TNF-α) expression is correlated with the progression of intervertebral disc degeneration (IVDD). Progranulin binding to tumor necrosis factor receptor (TNFR) and its derivative Atsttrin are effective for treating inflammatory arthritis. We hypothesize that Atsttrin has a protective effect in IVDD through different roles of TNFR receptor type 1 (TNFR1) and TNFR receptor type 2 (TNFR2) in degenerated discs.

Methods: IVDD models were established in TNFR1$^{-/-}$, TNFR2$^{-/-}$ mice and their control littermates. Nucleus Pulpous (NP) samples from human patients and IVDD murine models were evaluated by X-ray, micro-MRI, μCT, histological staining and immunofluorescence staining. NP cells isolated from wild-type (WT), TNFR1$^{-/-}$ and TNFR2$^{-/-}$ mice were treated with TNF-α or Atsttrin and then assayed by Western blotting, qRT–PCR, and ELISA.

Results: TNFR1 and TNFR2 expression was significantly elevated in the disc tissues of both human patients and IVDD murine models. TNFR1 knockout contributed to reduced disc degeneration. In contrast, TNFR2 knockout was associated with enhanced IVDD severity, including degraded cellular composition, increased cell apoptosis and elevated vertebral destruction. Atsttrin protected against IVDD in WT and TNFR1$^{-/-}$ mouse models but had no effect in TNFR2$^{-/-}$ IVDD models. Additionally, *in vitro* NP cell-based assays demonstrated that TNF-α-stimulated catabolism and Atsttrin-activated anabolism depended on TNFR1 and TNFR2, respectively.

Conclusion: TNFR1 is associated with the degenerative progression of IVDD, while TNFR2 contributes to the protective effect on the discs. Atsttrin protects against IVDD at least partially by inhibiting the TNFα/TNFR1 inflammatory/catabolic pathway and activating the TNFR2 protective/anabolic pathway.

The translational potential of this article: This study demonstrates that TNFR1 and TNFR2 have disparate roles in disc degeneration and hlights the potential use of Atsttrin as a therapeutic agent against IVDD in mice.

1. Introduction

Low back pain (LBP) is one of the most common age-related conditions causing functional disability and activity limitations [1–3]. Intervertebral disc degeneration (IVDD) is considered one of the strongly associated causes of LBP [4,5]. IVDD refers to a cascade that begins with changes to the cell microenvironment and progresses to structural breakdown and functional impairment [6,7]. This degenerative progress has been extensively characterized by molecular, morphological and biomechanical alterations to the discs and surrounding joint tissues [8].

IVDD is often associated with inflammatory cascades [9–12]. In particular, the expression and signaling of proinflammatory tumor necrosis factor alpha (TNF-α) are upregulated in degenerated discs [12–16]. Although TNF-α inhibitors (TNFIs) have been accepted as highly effective anti-inflammatory biologics, risks and limitations result in unsatisfactory therapeutic effects for up to 50% of patients [17–20]. Moreover, the efficacy of clinically available TNFI in LBP treatment remains controversial [21–26].

TNF-α interacts with two receptors, TNF receptor type 1 (TNFR1) and TNF receptor type 2 (TNFR2). TNFR1 is expressed in most cell types and is considered the primary receptor mediating TNF's proinflammatory effects, including activation of the transcription factors NF-κB and MAP kinases, leading to the transcription of proinflammatory cytokines. TNFR2 is primarily expressed in immune and endothelial cells as well as chondrocytes [27]. The roles of TNFR2 signaling in normal and degenerated tissues remain less well characterized, although accumulating evidence supports a protective role of TNFR2 signaling in some inflammatory conditions, particularly inflammatory arthritis [28]. Increasing evidence indicates that these two receptors play distinct roles in various pathophysiological processes, including neurodegeneration and inflammatory arthritis [27–31].

A prior global genetic screen led to the identification of TNFR as the preferential progranulin (PGRN)-associated receptor; PGRN and TNF-α bind to TNFR1 with comparable affinity, and PGRN acts as a naturally occurring antagonist of the TNF-α/TNFR1 interaction [27]. In contrast, PGRN interacts with TNFR2 at approximately 600-fold higher levels than TNF-α [27], and PGRN directly binds to and activates the TNFR2 protective pathway [32]. PGRN has been evaluated as a promising therapeutic target in various diseases, including common neurological diseases, inflammatory autoimmune diseases, cancer, tissue repair, and rare lysosomal storage diseases [33–37]. Despite the anti-inflammatory effects of PGRN, its multiple functions and oncogenic activity prohibit practical therapeutic implementation [38]. Accordingly, a PGRN derivative composed of half units of granulins A, C, and F plus linkers P3–P5 appears to be the "minimal" engineered molecule that retains binding affinity to TNFR2. This derivative, referred to as Atsttrin, lacks the oncogenic activity of PGRN but retains preventative and therapeutic efficacy in murine models of TNF-α-driven inflammatory disease [27]. However, the effect and mechanism of how Atsttrin plays a role in IVDD need to be clarified.

This study aimed to investigate the role of TNFR1 and TNFR2 in the course of IVDD and to determine whether Atsttrin has therapeutic prospects in the treatment of IVDD.

2. Materials and methods

2.1. Patient samples

Approval for the collection of patient disc samples was obtained from the Ethics Committee of Jiangyin Affiliated Hospital of Nanjing University of Chinese Medicine and performed in accordance with ethical standards. NP samples comprising the control group were collected from vertebral fracture patients without disc degeneration (n = 4). NP samples of the IVDD group were collected from lumbar disc herniation patients (Pfirrmann grade III and IV) (n = 4). Inflammatory cytokine and TNF receptor expression in these disc samples was detected by real-time qRTPCR analysis. All qRT–PCR amplifications were performed in triplicate, and the experiments were repeated at least three times.

2.2. Murine IVDD model

To further confirm the roles of the TNF receptor, we performed animal experiments. All animal studies were performed in accordance with institutional guidelines and with approval by the Institutional Animal Care and Use Committee of Southeast University. Animals were housed with ad libitum access to food and water under a 12-h light/dark cycle within a rodent barrier facility. The phenotype of mice was confirmed by genotyping when the mice were 4–6 weeks old. IVDD or sham surgery models were established in randomly allocated, experimentally native 12-week-old male C57BL/6 background wild-type (WT), TNFR1-knockout (TNFR1$^{-/-}$), TNFR2-knockout (TNFR2$^{-/-}$), and NF-κB reporter mice via needle puncture of caudal intervertebral discs in accordance with previously published reports [39,40]. Each group included 3 mice. Surgeries were performed under ketamine/xylazine-induced

general anesthesia (Ketaset 90 mg/kg body weight/xylazine 10 mg/kg body weight, intraperitoneal injection) in a sterile procedure room. In the IVDD surgery model groups, each mouse underwent disc puncture at the tail. A small sagittal skin incision was made from Co2 to Co6 to help locate the disc position for needle insertion in the tail. Subsequently, Co3–Co5 coccygeal discs were punctured using a 31G syringe needle. The syringe needle was inserted into the Co3–Co5 disc along the vertical direction and then rotated in the axial direction by 180° and held for 10 s. The puncture was made parallel to the end plates through the AF into the NP using a 31-G needle, which was inserted 1.5 mm into the disc to depressurize the nucleus. In the sham surgery model group (control group), only a small sagittal skin incision was made in each mouse tail. Macroscopic morphological changes to the intervertebral space were examined at 4 and 8 weeks after model induction by film X-ray and micro-MRI. Mice were sacrificed via CO$_2$ overdose followed by cervical dislocation at 4 or 8 weeks post model induction and processed for histological examination of morphological and molecular changes to intervertebral disc and vertebral tissues using H&E, Safranin O, TRAP and immunohistochemical staining. The expression of relevant anabolic and catabolic proteins in intervertebral discs and in vertebral bone at adjacent degenerative discs was further analyzed by immunofluorescence staining (IF), Western blot, and RT–PCR. Vertebral bone changes in adjacent degenerative discs were further analyzed by micro-CT (Siemens Inveon CT). Six mice from each genotype were employed for each experimental endpoint.

2.3. Hematoxylin-eosin (H&E) and immunohistochemical staining

The tail samples of mice were collected and incubated with 4% PFA in PBS overnight at 4 °C. Then, the tissues were washed with PBS, decalcified with 10% EDTA for 2–4 weeks, and embedded in paraffin. Midsagittal sections were obtained and stained with H&E and safranin O-fast green. The procedures were guided by a well-established protocol. The sections were examined under a light microscope (Axio Scope. A1, Zeiss, Oberkochen, Germany), and the lesion areas were measured by ImageJ (ImageJ 1.52a). H&E– and Safranin O-stained sections were scored across 5 categories of degenerative changes, with scores ranging from 5 points (1 in each category) for a normal disc to 15 points (3 in each category) for a severely degenerated disc. The five categories include the cellularity of the annulus fibrosis, the morphology of the anulus fibrosus, the border between the annulus fibrosis and nucleus pulposus, the cellularity of the nucleus pulposus, and the morphology of the nucleus pulposus.

For immunohistochemistry staining, sections were pretreated with 0.1% trypsin for 30 min at 37 °C. Sections were washed with PBS three times, followed by treatment with 0.25 U/ml chondroitinase ABC (Sigma–Aldrich) for 1 h and then 1 U/ml hyaluronidase (Sigma–Aldrich) for 1 h at 37 °C. To reduce nonspecific staining, sections were blocked at room temperature with 20% normal horse serum diluted in 3% BSA for 1 h. Without washing after blocking, TNFR1 and TNFR2 antibodies (1:200 dilution; DSHB) and aggrecan neoepitope antibodies (ab3208, 1:200 dilution; Abcam) were diluted in 20% normal horse serum with 3% BSA at 4 °C overnight. Sections were prepared for detection using the Vectastain Elite ABC kit following the manufacturer's guidelines at 25 °C for 1 h. Immunoreactivity was visualized using 0.5 mg/ml 3,3'-diaminobenzidine (DAB) in 50 mM Tris–HCl substrate, pH 7.8. Methyl green (1%) was used for counterstaining.

2.4. Film X-ray and MRI

Mice were euthanized with an intraperitoneal injection of 5 mg of pentobarbital sodium, and all mouse tails were harvested. First, we captured X-ray photos of these mouse tails using an X-ray machine in our lab. Midsagittal MRI images of all tail discs were acquired using micro-MRI (7-T Bruker Biospec 70/30) and qualitatively analyzed the MRI results according to the degenerative changes. The change in disc height

was evaluated by the disc height index (DHI) [40].

2.5. IVIS imaging

An IVIS spectrum imaging core was used according to the protocol (PerkinElmer IVIS Spectrum). The XGI-8 anesthesia system was used in conjunction with the IVIS Spectrum to anesthetize mice undergoing bioluminescent whole-body imaging. Four NF-κB reporter IVDD model mice were established via needle puncture of caudal intervertebral discs. Two IVDD model mice were g 100 μl of vehicle (sterile phosphate buffered saline, PBS) or Atsttrin (dosed at 2.5 mg/kg body weight [28]) via intraperitoneal injection once weekly beginning from the day of model induction until sacrifice at 4 weeks post model induction. Another two mice as the control group underwent sham surgery.

2.6. NP cells culture

The mouse disc tissues were isolated from tail discs using a stereotaxic microscope, washed twice with phosphate-buffered saline (PBS), cut off the annulus fibers (AF) at the outside of each disc tissue, and then cut into 2–3 pieces. NP cells were released from these NP tissues by incubation with 0.25 mg/ml type II collagenase (Invitrogen, Carlsbad, CA, USA) for 12 h at 37 °C in Dulbecco's modified Eagle medium (DMEM; Gibco, Grand Island, NY, USA). NP cells were seeded at 1×10^6 cells in 12-well plates and cultured in F12 basal medium supplemented with 2.5% Matrigel, 10% fetal bovine serum plus 2.5 mg/mL L-ascorbic acid-2-phosphate (Sigma). The medium was changed twice per week for the duration of cell pellet culture.

2.7. qRT–PCR

qRT–PCR was performed to measure mRNA expression. The mice were euthanized, and the tails were cut off. The discs of these tails were separated, snapped into liquid nitrogen, and transferred to −80 °C until use. The cultured cells were also collected. Total RNA was isolated with TRIzol Reagent (Ambion, Life Technologies, Carlsbad, CA, USA) from disc tissues or cultured cells according to the manufacturer's instructions. RNA quantity was determined using a Nanodrop spectrophotometer (Thermo Scientific, Waltham, MA, USA). Quantification of mRNA expression was performed on the StepOnePlus Real-Time PCR System (Life Technologies) using TaqMan Gene Expression Assays (Life Technologies) specific for TNF, TNFR1, TNFR2, MIP-1α, MCP-1, IFN-γ, IL-6, IL-1α, Aggrecan, Collagen II, TRAP, Cathepsin, BAX, Bcl-2 and MMP-13. Data were normalized to the internal control, GAPDH. The primers for specific amplification of murine genes are as follows:

5′-GACGTGGAACTGGCAGAAGAG-3′ and 5′-TTGGTGGTTTGTGAG TGTGAG -3′ for TNF-α; 5′-CCGGGAGAAGAGGGATAGCTT-3′ and 5′-TCGGACAGTCACTCACCAAGT-3′ for TNFR1; 5′-ACACCCTACAAA CCGGAACC-3′ and 5′-AGCCTTCCTGTCATAGTATTCCT -3′ for TNFR2;
5′-ACAGGCTCTTGACCAGGCATA-3′ and 5′-ACTTAACAGTTCGCCG AATTTGA -3′ for MIP-1;
5′-CATAGCAGCCACCTTCATTCC-3′ and 5′-TCTCCTTGGCCACAAT GGTC-3′ for MCP-1;
5′-TCGGTAACTGACTTGAATGTCCA-3′ and 5′-TCGCTTCCCTGTTTTA GCTGC-3′ for IFN-γ;
5′-GGCCCTTGCTTTCTCTTCG-3′ and 5′-ATAATAAAGTTTTGATT ATGT-3′ for IL-6;
5′-AATCTCACAGCAGCACATCA-3′ and 5′-AAGGTGCTCATGTCCT-CATC-3′ for IL-1α;
5′-AATGCTGGTACTCCAAACCC-3′ and 5′-CTGGATCGTTATCCAG-CAAACAGC-3′ for Aggrecan;
5′-ACTAGTCATCCAGCAAACAGCCAGG-3′ and 5′-TTGGCTTTGGG AAGAGAC-3′ for Collagen II;

5′-TCCCCTGGTATGTGCTGG-3′ and 5′-GCATTTTGGGCTGCTGA-3′ for TRAP;
5′-TGGGAGCTGTGGAAGAAGAC-3′ and 5′-TTTCATCCTGCCCCACA-TAC-3′ for Cathepsin;
5′-CCCGAGAGGTCTTTTTCCGAG-3′ and 5′-CCAGCCCATGATGGTT CTGAT-3′ BAX;
5′-GAGCCATCTCAGTGTGTGGAG-3′ and 5′-GCCAGCATTGCCATAA AAGAGTC-3′ for Bcl-2;
5′-ACTTTGTTGCCAATTCCAGG-3′ and 5′-TTTGAGAACACGGGGAA-GAC-3′ for MMP-13;
and 5′-AGAACATCATCCCTGCATCC-3′ and 5′-AGTTGCTGTTGAAG TCGC-3′ for GAPDH. Melting curve analysis was used to verify the PCR product. Each experiment was repeated three times.

2.8. Immunofluorescence

The frozen sections were first penetrated with 0.1% Triton X-100 for 10 min and then blotted with 5% donkey serum in PBS for 30 min. The sections were then incubated with primary antibodies overnight at 4 °C and subsequently rinsed with PBS and incubated with secondary antibodies at room temperature for 1 h. After rinsing with PBS 3 times, the slides were mounted with Vectashield mounting medium with DAPI (H-1200, Vector Laboratories, Burlingame, CA, USA). The slides were subsequently screened under an immunofluorescence microscope (Axio Scope. A1, Zeiss, Oberkochen, Germany).

2.9. Assays to examine the therapeutic effects of atsttrin in IVDD in vivo

To investigate the protective effects of Atsttrin on IVDD, IVDD model mice were administered 100 μl of vehicle (sterile phosphate buffered saline, PBS) or Atsttrin (dosed at 2.5 mg/kg body weight [28]) via intraperitoneal injection once weekly beginning from the day of model induction until sacrificial at 4 or 8 weeks post model induction. Six mice of each genotype were employed for each experimental endpoint.

2.10. Assays to examine the catabolic and anabolic activity of TNF-α and atsttrin in nucleus pulpous cells in vitro

We separated the nucleus pulpous from WT, TNFR1$^{-/-}$ and TNFR2$^{-/-}$ mice separately. Then, NP cells were isolated via incubation of intervertebral nucleus pulpous tissues in DMEM for 5 days. Cells were then seeded into a six-well plate and treated with TNF-α (10 ng/ml) or Atsttrin (100 ng/ml) for further experiments [21]. At the indicated time points, NP cells were harvested for analysis by WB and RT–PCR. Culture media was collected, and the levels of the secretory inflammatory cytokines IL-6 and IL-1β were assessed by ELISA.

2.11. Statistical analysis

ImageJ (ImageJ 1.52a) was implemented for image quantification as necessary. For statistical analysis, GraphPad Prism 7 Software (GraphPad Software, San Diego, CA, USA) was used. A significant difference between two experimental groups was identified by multiple t tests, including one per row. To compare the significant differences among multiple groups, we used the mean ± SD and one-way analysis of variance. A p value < 0.05 was considered statistically significant.

3. Results

3.1. TNFR1 and TNFR2 are significantly upregulated in both human and mouse degenerative disc tissues

Transcript levels of various inflammatory cytokines known to be involved in inflammatory/degenerative diseases in nucleus pulposus samples collected from patients with spinal trauma (vertebral fracture patients without disc degeneration, n = 4) and disc degeneration (grade

C IVDD patients, n = 4) were measured by real-time qPCR. Among the cytokines screened, TNF-α, TNFR1 and TNFR2 were significantly increased in biopsies from patients with degenerative nucleus pulposus compared to control tissues (Fig. 1A and B). Similarly, we sought to examine the effect of IVDD on the expression levels of TNFR1 and TNFR2 in IVDD model mice. As shown in Fig. 1C & D, the expression levels of TNFR1 and TNFR2, detected by immunohistochemistry, were also significantly elevated in the nucleus pulposus of the murine IVDD group compared to the control group.

3.2. Deficiency of TNFR1 and TNFR2 is associated with decreased and enhanced IVDD severity, respectively

Histological examination and quantitative analysis were performed on mouse disc samples at four and eight weeks post-IVDD surgery. H&E staining (Fig. 2A&B, S4) showed pathological changes in discs in all IVDD mice with three different genetic backgrounds at 4 and 8 weeks; degenerative changes were particularly pronounced in TNFR2$^{-/-}$ mice at 8 weeks postsurgery. H&E and Safranin O staining showed reduced disc degeneration in TNFR1$^{-/-}$ mice compared to WT and TNFR2−/− mice, with greater maintenance of the distinct nucleus pulposus morphology compared to loss of the boundary with the annulus fibrosus (Fig. 2A–D). Loss of the distinct annulus fibrosus morphology was more severe in TNFR2$^{-/-}$ IVDD discs, where chondrocytes accounted for approximately 75% of the annulus fibrosus cells (Fig. 2C&D). TNFR2$^{-/-}$ IVDD discs showed more bulged, ruptured or serpentine fibers in the annulus fibrosus; a moderate to severe decrease in the number of NP cells; and rounded or irregularly shaped NP morphology (Fig. 2C&D). X-ray images of IVDD mouse tails revealed milder and more severe decreases in the space of the intervertebral disc area and increased ossification in the endplates of TNFR1$^{-/-}$ and TNFR2$^{-/-}$ mice compared to WT mice

(Fig. 2E&F, S6). These changes were confirmed by micro-MRI scanning under general anesthesia. MRI results showed decreased disc signals in all groups following needle puncture, with a noticeably greater reduction in signal in TNFR2$^{-/-}$ IVDD mice (Fig. 2G&H). Collectively, these findings showing that loss of TNFR1 protects against while loss of TNFR2 accelerates the progression of IVDD suggest that TNFR1 and TNFR2 may mediate destructive and protective processes in the pathogenesis of IVDD, respectively.

3.3. Loss of TNFR1 and TNFR2 leads to significantly distinctive changes in cell matrix composition in IVDD

We performed a series of histological assays to examine changes in cell matrix composition following IVDD model establishment. MMP13 is one of the main cytokines involved in intervertebral disc degeneration. As revealed by immunofluorescence analysis (Fig. 3A), matrix metalloproteinase MMP13 expression was increased in the degenerated discs. More robust expression of MMP13 was observed in TNFR2$^{-/-}$ IVDD than in TNFR1$^{-/-}$ and WT mice (Fig. 3A&B). In addition, the absence of TNFR1 attenuated the expression of MMP13 in IVDD discs compared with WT mice. Fig. 3C shows immunohistochemistry staining of the catabolic marker Aggrecan degenerative-generated neoepitope in intervertebral disc samples from sham and IVDD groups of different genotypes. The corresponding quantitative analysis (Fig. 3D) demonstrated significantly elevated signaling in the TNFR2$^{-/-}$ group relative to the WT or TNFR1$^{-/-}$ groups. Primary components comprising the disc, Collagen 2 and Aggrecan, were decreased at mRNA expression levels in degenerated discs, especially in TNFR2$^{-/-}$ mice (Fig. 3E&F), and the decrease in these two markers was less pronounced in TNFR1−/− mice than in WT mice. These results illustrate increased catabolic activities and reduced expression of anabolic markers in all degenerative discs. TNFR2
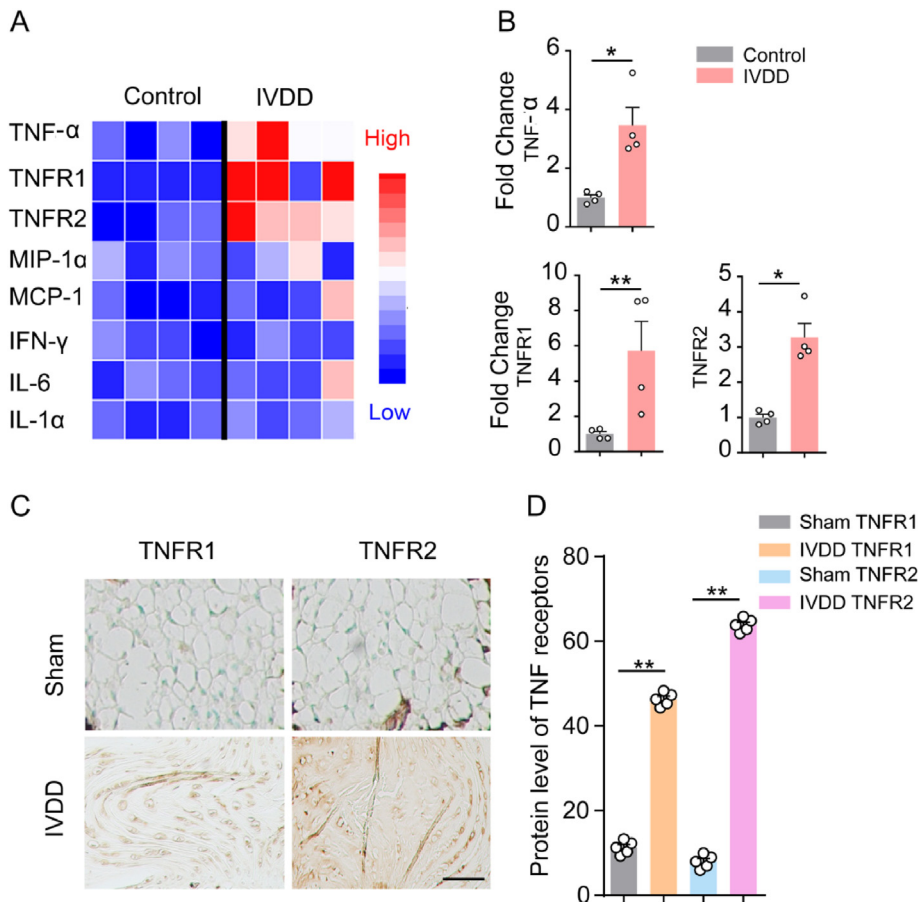

Figure 1. The levels of TNFR1 and TNFR2 are elevated in human and mouse degenerative disc tissues. A. A heat plot representation of real-time PCR mRNA expression of inflammatory cytokines and receptors in human control and IVDD intervertebral discs. TNF-α, TNFR1, TNFR2, and IL-1α mRNA were significantly increased in degenerative disc group (n = 4) relative to control (n = 4). B. Quantitative analysis of Fig. 1A. C. In the IVDD mice models, the degenerated intervertebral disc tissues (n = 5) exhibited higher expressions of TNFR1 and TNFR2 relative to sham controls (n = 5) as detected by immunohistochemistry. D. Quantitative analysis of (*p < 0.05, **p < 0.01).
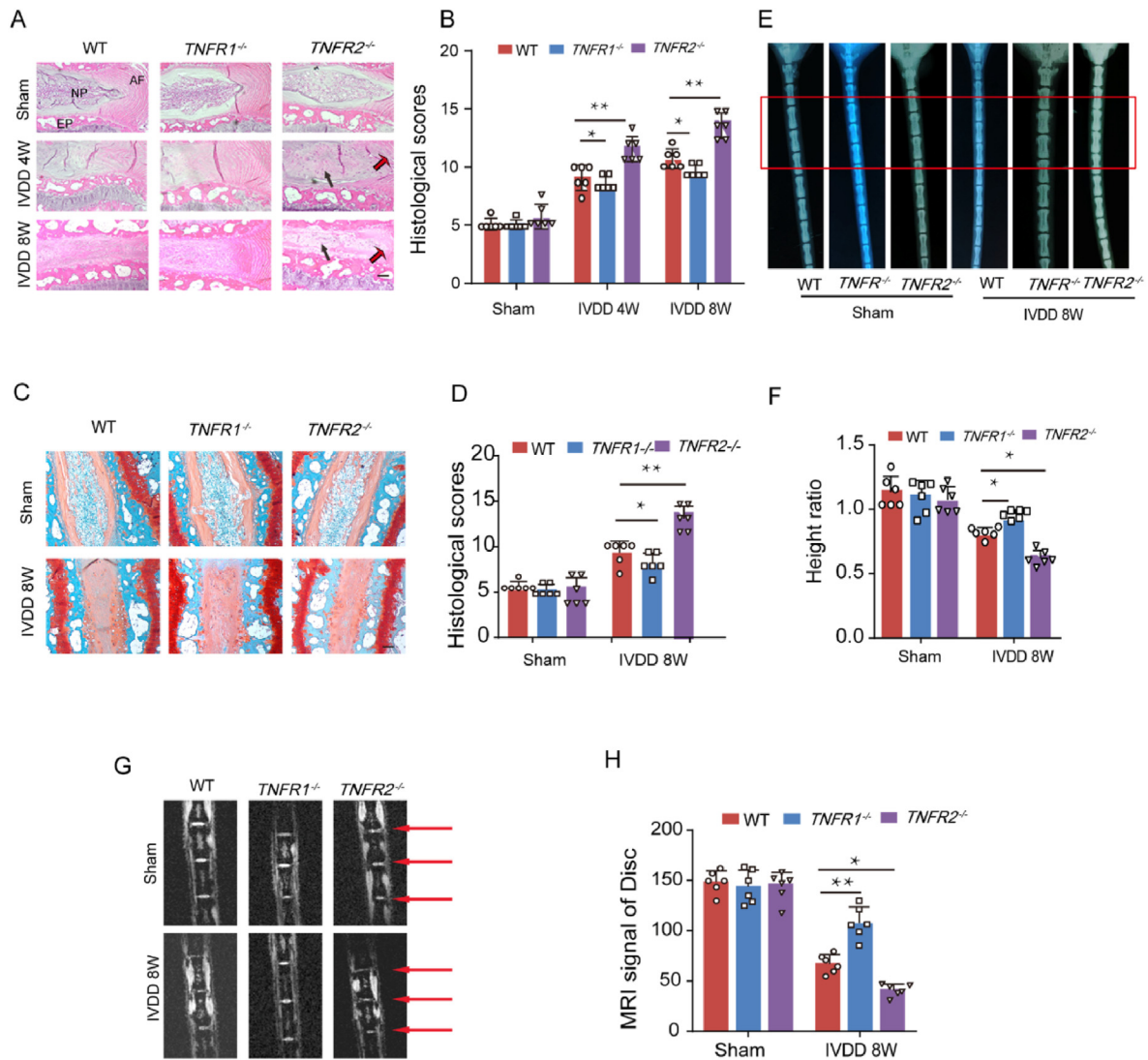
Figure 2. Loss of TNFR1 and TNFR2 protects against and accelerates the disc degeneration, respectively. A. Mice discs were collected and stained with H&E after 4 weeks and 8 weeks of needle puncture induced IVDD. Black arrows indicated the nucleus pulposus cells. Red arrows showed the inward bulging, ruptured or serpentine fibers. B. Histological score of disc was measured according to the HE staining results (Fig. 2 A). C. Safranin O staining of discs without needle puncture and after needle puncture for 8 weeks. D. Histological scores according to the Safranin O staining (Fig. 2C). E. 8 weeks post-needle puncture to induce IVDD, TNFR2$^{-/-}$ mice have less intervertebral disc space on X-ray images relative to WT and TNFR1$^{-/-}$ mice (model discs are highlighted in the red rectangle). F. Quantitative analysis of the x-ray changes on degenerated intervertebral space height (height ratio = the height of needle punctured discs (intervertebral space)/the height of adjacent discs without do needle puncture. G. MRI examination of the intervertebral disc of different genetic background. H. Qualitative analysis of MRI signals of discs (NP = nucleus pulposus, AF = annulus fibrosus, EP = endplate, Scale bars = 50 μm, data were presented as mean ± SD, n = 6 per group, *p < 0.05,**p < 0.01.).

deficiency led to more severe degenerative changes with regard to these markers of cellular metabolism compared with TNFR1$^{-/-}$ and WT mice, while TNFR1 deficiency resulted in ameliorated degenerative changes relative to WT mice.

3.4. Loss of TNFR1 and TNFR2 leads to less and more local vertebral bone destruction in IVDD, respectively

In clinical intervertebral disc degeneration cases, not only are the discs affected, but the adjacent vertebrae also exhibit degenerative changes. Accordingly, we investigated local changes in the vertebral bone of IVDD model mice. Interestingly, we found that loss of TNFR1 and TNFR2 led to a significant decrease and increase in osteoclasts in vertebral bodies adjacent to degenerative discs, respectively. Tartrate-resistant acid phosphatase (TRAP) staining revealed an increase in osteoclast number at the endplate adjacent to degenerative discs in all three different genetic background mice with IVDD; however, evidence

for enhancement of osteoclastogenesis was more pronounced in the TNFR2$^{-/-}$ group (Fig. 4A&B, S7), and TNFR1$^{-/-}$ IVDD discs had fewer TRAP-positive cells than WT IVDD discs. Correspondingly, real-time qPCR results showed that the mRNA expression levels of TRAP and Cathepsin K were significantly downregulated and upregulated in the TNFR1$^{-/-}$ and TNFR2$^{-/-}$ IVDD groups, respectively, compared to WT mice with IVDD (Fig. 4C&D).

To further assess vertebral bone quality in our IVDD model mice, we performed micro-CT scanning and quantified the bone mineral density (BMD) of the vertebra adjacent to the degenerated discs. The TNFR2$^{-/-}$ IVDD group had the lowest vertebral BMD among all three groups (Fig. 4E&F). These results indicate the development of osteoporosis in the vertebra adjacent to the degenerative disc and, more importantly, that TNFR2$^{-/-}$ IVDD model mice exhibit a more severe loss of BMD than WT and TNFR1$^{-/-}$ mice. Taken together, these results highlight clear differences in bone quality at degenerative disc-adjacent vertebrae and further indicate that TNFR1 and TNFR2 play opposite roles in disc
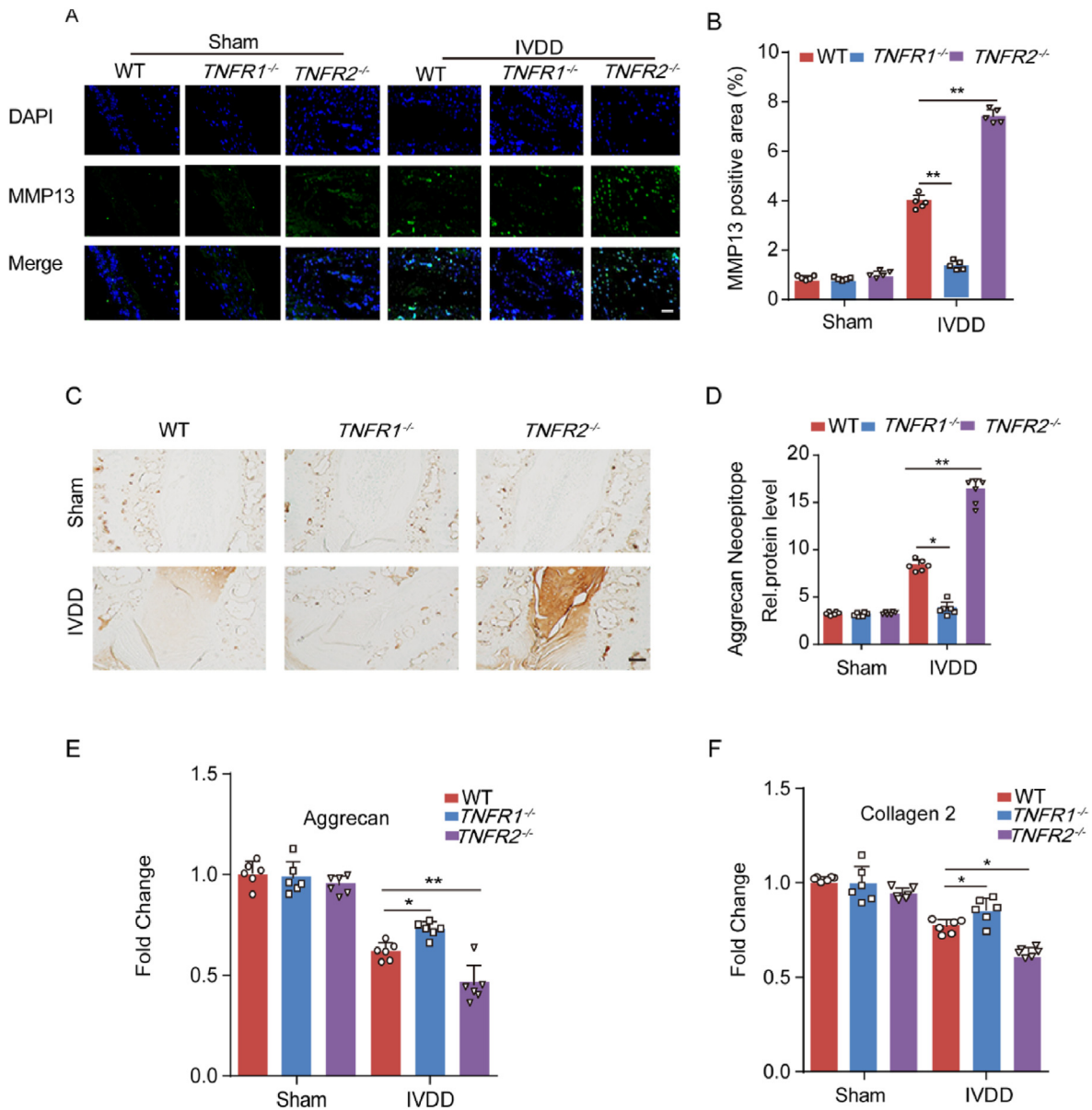
Figure 3. Deficiency of TNFR1 and TNFR2 leads to significant changes of cellular composition in needle-puncture induced IVDD. A. By immunofluorescence analysis of the discs, more robust expression of MMP13 was observed in TNFR2−/− IVDD mice than that in TNFR1−/− and WT mice. B. Quantification of A. C. Immuno-histochemical staining for aggrecan neoepitope showed increased expression level in TNFR2−/− mice. D. Quantification of C. E, F. real time qPCR detection of mRNA levels of aggrecan and collagen II (n.s. = not significant, *p < 0.05, **p < 0.01, Bar = 50 μm, n = 6, data were presented as mean ± SD).

degeneration by prompting and inhibiting the loss of vertebral bone near degenerated discs, respectively.

3.5. Deficiency of TNFR1 and TNFR2 is associated with decreased and increased apoptosis in degenerated discs, respectively

Cell apoptosis plays an important role in various degenerative diseases, including IVDD. We next sought to examine whether TNFR1 and TNFR2 also affected disc cell apoptosis in IVDD. We first performed an apoptosis assay with an Annexin V approach. Increased apoptosis in all degenerated discs with different genotypes was observed. Additionally, significantly reduced apoptosis was observed in TNFR1$^{-/-}$ IVDD mice compared with WT IVDD mice, whereas the most drastic increase in apoptosis was observed in TNFR2$^{-/-}$ IVDD mice (Fig. 5 A&B). Furthermore, real-time qPCR analysis of intervertebral disc tissue following needle puncture-induced IVDD showed increased pro-apoptotic Bax expression and decreased anti-apoptotic Bcl-2 expression in all IVDD

model mice compared to sham groups. Compared to those in the WT IVDD group, deletion of TNFR1 reduced Bax but increased Bcl-2 expression, whereas ablation of TNFR2 increased Bax but decreased Bcl-2 expression in the discs of corresponding IVDD mice (Fig. 5C).

3.6. Atsttrin protects against IVDD in WT and TNFR1−/− mice but largely loses its protective effects in TNFR2−/− mice

Our previous studies demonstrated that Atsttrin plays a protective function in inflammatory diseases such as arthritis without any significant side effects [28]. To further determine whether Atsttrin also has therapeutic effects on IVDD, we established a needle puncture-induced IVDD model in NF-κB reporter mice and administered Atsttrin through weekly intraperitoneal injection for four weeks. IVIS imaging (PerkinElmer IVIS Spectrum) illustrated significantly reduced NF-κB-mediated luciferase signal activation in the Atsttrin-treated group relative to control mice with needle puncture-induced IVDD (Fig. 6A&B). To further
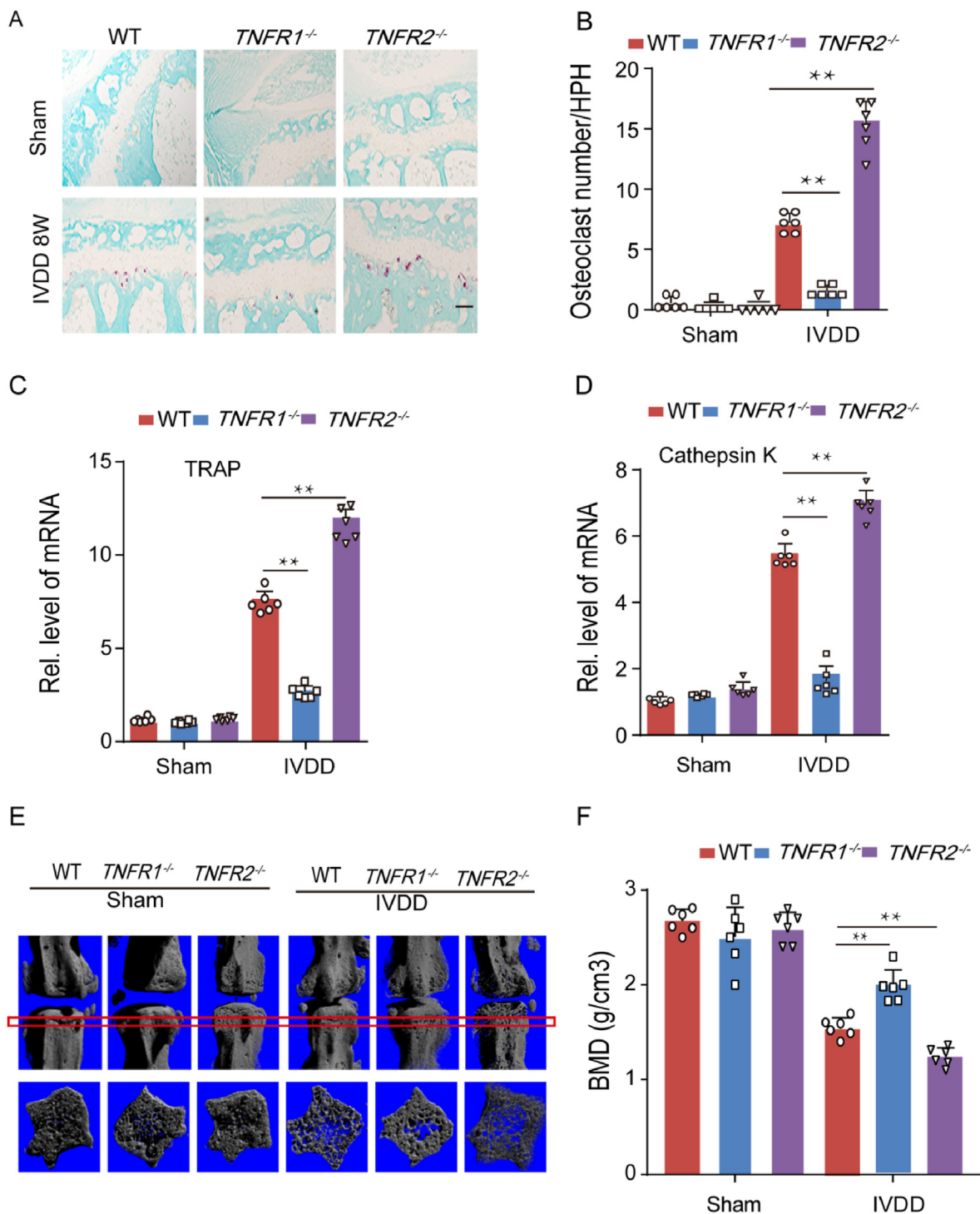
Figure 4. Loss of TNFR1 and TNFR2 leads to less and more local vertebral bone destruction, respectively, in the tails of needle-puncture induced IVDD mice. A. TRAP staining of TNFR2$^{-/-}$, TNFR1$^{-/-}$ and WT vertebra adjacent to the degenerative disc. B. Quantification of A. C, D. real time qPCR analysis of mRNA expression of TRAP and Cathepsin K. E. Micro-CT reconstructed the vertebral bone near to the disc and showed some bone loss in IVDD groups. F. The bone mineral density of the vertebra adjacent to the degenerated disc further confirmed more local vertebral bone destruction in TNFR2$^{-/-}$ IVDD mice relative to WT and TNFR1$^{-/-}$ mice (*p < 0.05, **p < 0.01, Bar = 50 μm, n = 6, data were presented as mean ± SD).

determine the dependence of Atsttrin therapeutic effects on TNFRs in IVDD, an IVDD model was established in WT, TNFR1$^{-/-}$ and TNFR2$^{-/-}$ mice followed by treatment with Atsttrin for four weeks. Histological analyses showed significant improvement of disc degeneration scores in Atsttrin-treated TNFR1$^{-/-}$ and WT mice relative to the PBS injected IVDD mice; however, no therapeutic effect of Atsttrin was observed in TNFR2$^{-/-}$ IVDD mice and histological scores of disc degeneration were statistically indistinguishable from those of PBS treated IVDD mice (Fig. 6C&D). MRI scanning also demonstrated that Atsttrin attenuated the narrowing of the intervertebral disc space and loss of NP signals in TNFR1$^{-/-}$ and WT mice but did not appear in TNFR2$^{-/-}$ mice (Fig. 6E&F). Taken together, these results indicate that Atsttrin protects against IVDD and that its therapeutic effects in IVDD mainly depend on the TNFR2 protective pathway.
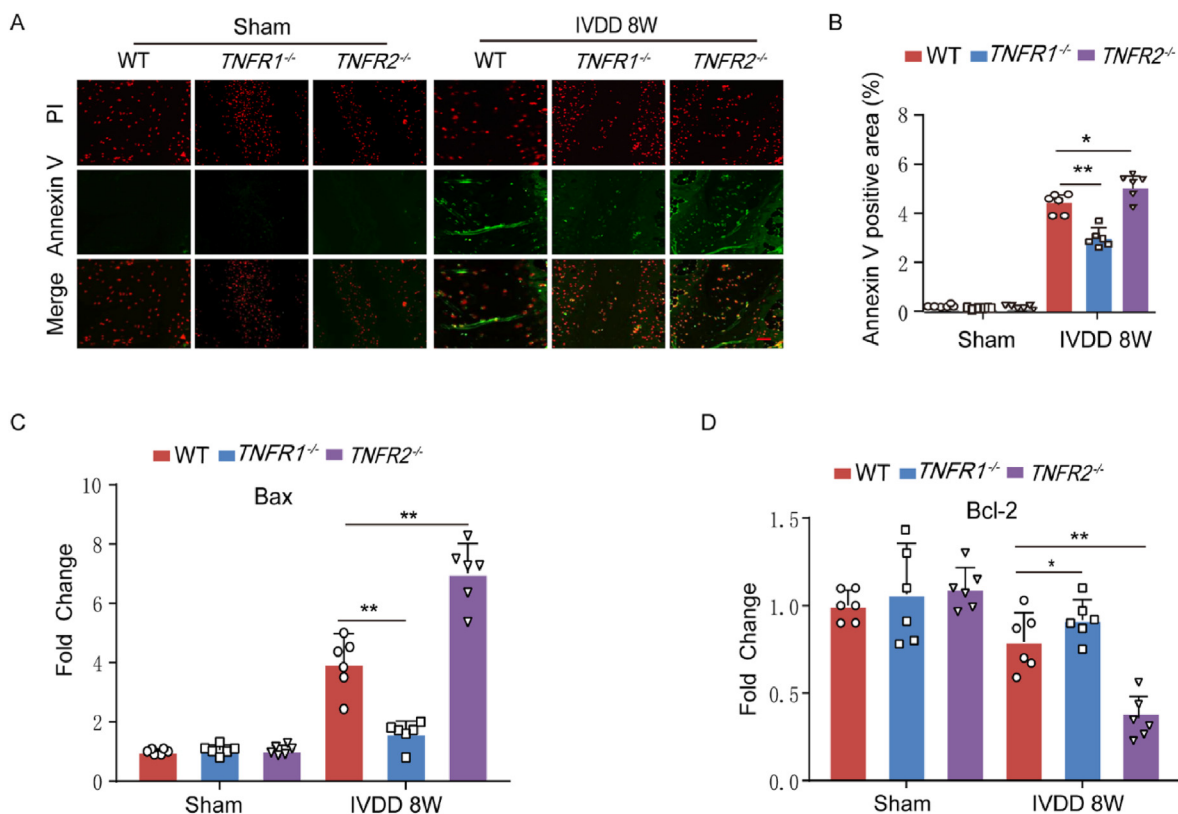
Figure 5. Apoptosis is decreased in the degenerated discs of TNFR1$^{-/-}$ mice whereas significantly increased in TNFR2$^{-/-}$ mice. A. Annexin V analysis showed the apoptosis levels in the degenerative discs of different genotype mice. Among these mice, TNFR2$-/-$ IVDD mice showed more apoptosis than which in TNFR1$-/-$ and WT mice. B. Quantification of A. C. and D. Expressions of Bax and Bcl-2 in the discs of sham and IVDD mice were measured by real time qPCR analysis (*p < 0.05, **p < 0.01, n = 6, data were presented as mean ± SD).

4. Discussion

The intervertebral disc plays an important 'spacer' and 'stabilizer' role in the optimal anatomical and biomechanical function of the spine. IVDD is a common degenerative disease correlated with aging that is closely related to low back pain, which contributes to disability, decreased quality of life in patients, and increased heath care costs [41–43]. As a central inflammatory molecule, TNF-α expression has already been examined in human degenerated intervertebral discs [10, 44–47], and anti-TNF therapies have shown therapeutic promise in *in vitro* models of disc degeneration [44,45]. Although native disc cells express very few TNF receptors, we demonstrated that the expression of both TNFR1 and TNFR2 is significantly upregulated in degenerated human discs relative to nondegenerated controls. We also established a needle puncture-induced IVDD model in C57BL/6 WT mice and similarly found that both TNFR1 and TNFR2 were increased in these IVDD mice. To distinguish the roles of TNFR1 and TNFR2 in inflammatory signaling, key mediators of anabolic and catabolic cellular responses were monitored following *in vitro* treatment of disc cells isolated from WT, TNFR1$^{-/-}$ and TNFR2$^{-/-}$ mice with TNF-α or Atsttrin, an engineered protein composed of three TNFR-binding fragments of PGRN [28]. From these results, we demonstrated that the activation of phosphorylated p65 (p-p65) by TNF-α largely depends on TNFR1, while Atsttrin's anabolic effect mainly depends on TNFR2 in disc cells.

To further confirm the respective roles of TNFR1 and TNFR2 in degenerative discs *in vivo*, we established an IVDD model in WT, TNFR1$^{-/-}$ and TNFR2$^{-/-}$ mice. Compared with all three sham conditions, IVDD model establishment was associated with obviously increased catabolic activity and reduced anabolic activity in disc tissues. These changes in catabolic and anabolic markers illustrated an overall protective effect of TNFR1 deficiency and detrimental effects of TNFR2

deficiency on IVDD progression. MMP13 and the intermediate degradation product of aggrecan were increased in each group of IVDD mice, although TNFR2 deficiency was associated with the most dramatic increases. qRT–PCR further confirmed that the expression of collagen 2 and aggrecan, key components of disc composition, was downregulated in IVDD mice, with the most significant downregulation in TNFR2$^{-/-}$ mice.

Apoptosis plays an important role in many degenerative diseases, and the individual contributions of TNFRs to TNF-induced apoptosis may be cell type- and pathology-dependent [48]. In disc degeneration, we found that loss of TNFR2 accelerated cell apoptosis, as assessed through Annexin V staining and qRT–PCR analysis. In patients, mild to severe bone loss is also a common feature of vertebrae adjacent to degenerated discs. Interestingly, we also found enhanced osteoclast activity and reduced bone mineral density, as assessed by TRAP staining and microCT, respectively, in IVDD model mice with three different genetic backgrounds. Compared to WT IVDD mice, TNFR1$^{-/-}$ mice showed less osteoclast staining and less BMD loss, while the opposite trend was observed in TNFR2$^{-/-}$ mice. These results suggest that TNF receptors are also involved in the cellular apoptosis and intervertebral bone loss associated with IVDD and that TNFR1 and TNFR2 may play opposite roles in these pathological processes. These results suggest that the metabolic processes of nucleus pulposus cells and surrounding bone cells change to varying degrees during IVDD. The inflammatory response may promote apoptosis and osteoclast activity to varying degrees.

Importantly, the *in vivo* limitations of the application of TNF inhibition against IVDD may be attributable to simultaneous nonselective blockade of protective TNFR2-mediated activity. For instance, the TNF inhibitor etanercept (Enbrel) is a fusion soluble TNFR2 extracellular protein and works by binding to and blocking TNF-α, but it may also bind to and inhibit other TNFR2-binding molecules (e.g., PGRN) [28], resulting in nonspecific blockade of TNF-α proinflammatory signaling,
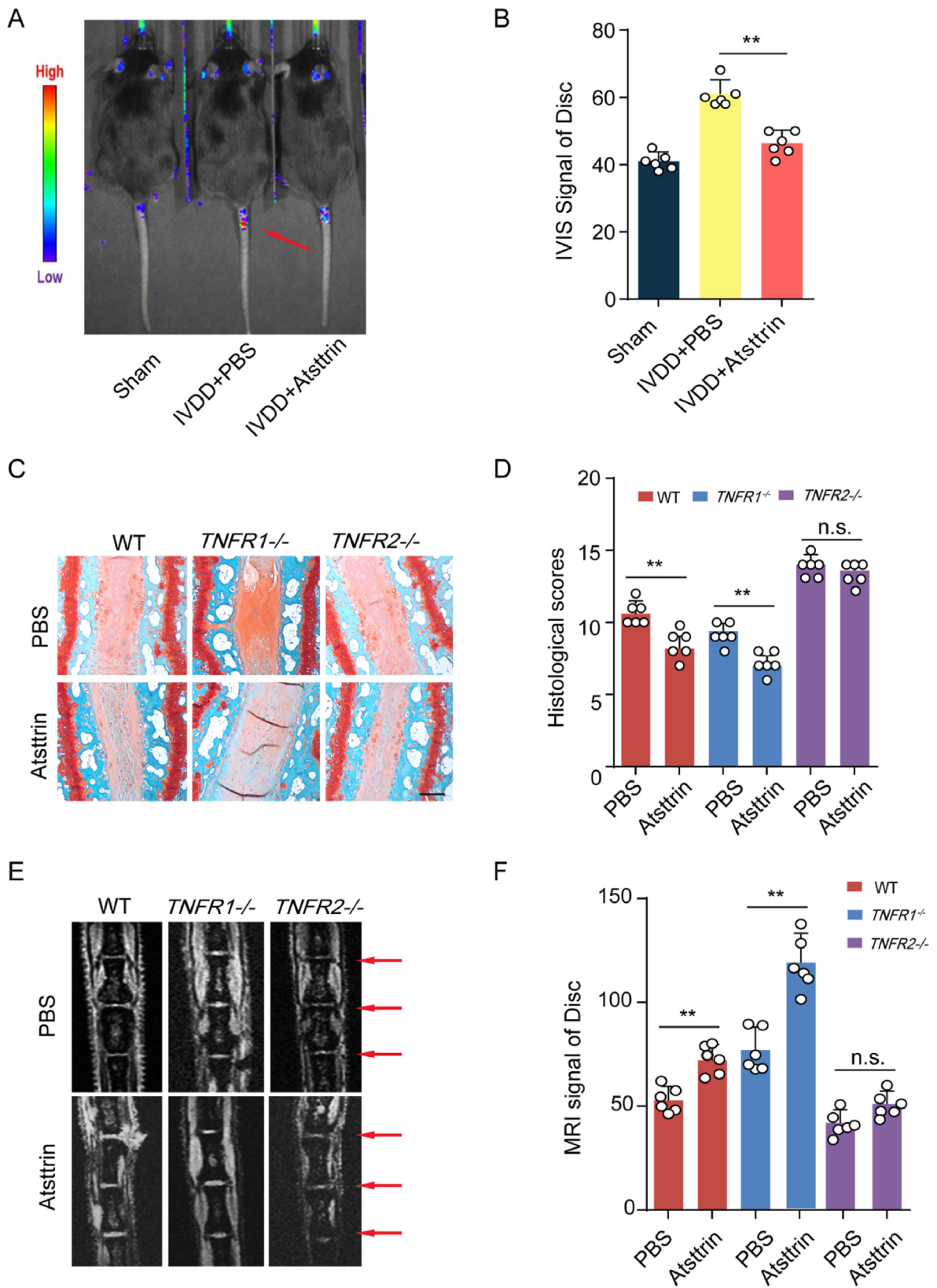
Figure 6. Atsttrin has therapeutic effects on needle-puncture induced IVDD mice. A. IVIS showed that Atsttrin can attenuate the inflammatory signal in IVDD model discs in NF-κB reporter mice. Red arrow indicates elevated signal in PBS-treated IVDD mice. B. Quantification of A. C. Safranin O staining on IVDD model discs of indicated genotype with or without Atsttrin treatment. D. Histological degeneration scores. E. MRI scanning. Red arrows indicate attenuated IVD space in TNFR2$^{-/-}$ mice. F. Quantification of E (n.s. = not significant, *p < 0.05, **p < 0.01, Bar = 50 μm, n = 6, data were presented as mean ± SD).

which may also be a reason for the controversial effects of TNFI on LBP as well as the lack of efficacious TNF-targeting agents for IVDD. Our findings that loss of TNFR1 can protect against while loss of TNFR2 can accelerate the needle puncture-induced disc degeneration model suggest that a new therapeutic strategy implementing selective interactions with TNF receptors may hold promise in addressing IVDD. In our previous studies, we demonstrated that Atsttrin, which binds to TNFR2 with a much higher binding affinity than TNF-α, exerts protective and therapeutic effects in inflammatory disease [28]. To determine whether Atsttrin has therapeutic effects in IVDD and the molecular mechanisms involved, we treated WT, TNFR1$^{-/-}$, and TNFR2$^{-/-}$ IVDD mice with weekly systemic Atsttrin administration for four weeks. We found that Atsttrin could effectively attenuate disc degeneration in WT and TNFR1$^{-/-}$ IVDD mice. Intriguingly, Atsttrin largely lost its protective function against IVDD progression in the absence of TNFR2. Overall, this evidence suggests that TNFR2 mediates the local homeostasis of disc tissues and maintains the capacity for survival and regeneration of disc tissue, but the possible mechanism of TNFR2's beneficial and protective effect on IVDD needs further study.

In summary, our study demonstrates that TNFR1 and TNFR2 have disparate roles in disc degeneration and that TNFR2 plays a beneficial and protective role in the intervertebral disc and vertebral bone. In addition, Atsttrin has therapeutic effects against IVDD in mice, and these effects may primarily depend on the presence of TNFR2.

Author contributions

S.Wang and G. Sun, designed and performed experiments, collected and analyzed data, and co-wrote the paper. P.Fan, L.Huang and Y.Chen assisted with experiments, and collected and analyzed data. C.Chen designed and supervised this study, analyzed data, and wrote and edited the manuscript.

Funding

Declaration of competing interest

None declared.

Acknowledgement

References

[1] George Steven Z, Fritz Julie M, Silfies Sheri P, et al. Interventions for the management of acute and chronic low back pain: revision 2021. J Orthop Sports Phys Ther 2021;51:CPG1–60 [eng].

[2] Leipold E, Liebmann L, Korenke GC, Heinrich T, Giesselmann S, Baets J, et al. A de novo gain-of-function mutation in SCN11A causes loss of pain perception. Nat Genet 2013;45(11):1399–404 [eng].

[3] Sarah Koumtouzoua, Higgins Stacy. Evaluating and managing the patient with back pain. Med Clin North Am 2021;105:1–17 [eng].

[4] Zhang S, Hu B, Liu W, Wang P, Lv X, Chen S, et al. The role of structure and function changes of sensory nervous system in intervertebral disc-related low back pain. Osteoarthritis Cartilage 2021;29:17–27 [eng].

[5] Smith M, Davis MA, Stano M, Whedon JM. Aging baby boomers and the rising cost of chronic back pain: secular trend analysis of longitudinal Medical Expenditures Panel Survey data for years 2000 to 2007. J Manip Physiol Ther 2013;36(1):2–11 [eng].

[6] Chou D, Samartzis D, Bellabarba C, Patel A, Luk KD, Kisser JM, et al. Degenerative magnetic resonance imaging changes in patients with chronic low back pain: a systematic review. Spine (Phila Pa 1976) 2011;36(21 Suppl):S43–53 [eng].

[7] Livshits G, Popham M, Malkin I, Sambrook PN, Macgregor AJ, Spector T, et al. Lumbar disc degeneration and genetic factors are the main risk factors for low back pain in women: the UK Twin Spine Study. Ann Rheum Dis 2011;70(10):1740–5 [eng].

[8] Mern Demissew Shenegelegn, Walsen Tanja, Beierfuß Anja, Thomé Claudius. Animal models of regenerative medicine for biological treatment approaches of degenerative disc diseases. Exp Biol Med 2021;246:483–512 [eng].

[9] Molinos M, Almeida CR, Caldeira J, Cunha C, Goncalves RM, Barbosa MA. Inflammation in intervertebral disc degeneration and regeneration. J R Soc Interface 2015;12(108):20150429 [eng].

[10] Navone SE, Marfia G, Giannoni A, Beretta M, Guarnaccia L, Gualtierotti R, et al. Inflammatory mediators and signalling pathways controlling intervertebral disc degeneration. Histol Histopathol 2017;32(6):523–42 [eng].

[11] Khan AN, Jacobsen HE, Khan J, Filippi CG, Levine M, Lehman Jr RA, et al. Inflammatory biomarkers of low back pain and disc degeneration: a review. Ann N Y Acad Sci 2017;1410(1):68–84 [eng].

[12] Risbud MV, Shapiro IM. Role of cytokines in intervertebral disc degeneration: pain and disc content. Nat Rev Rheumatol 2014;10(1):44–56 [eng].

[13] Johnson ZI, Schoepflin ZR, Choi H, Shapiro IM, Risbud MV. Disc in flames: roles of TNF-alpha and IL-1beta in intervertebral disc degeneration. Eur Cell Mater 2015;30: 104–16. discussion 16-7. [eng].

[14] Johnson ZI, Schoepflin ZR, Choi H, Shapiro IM, Risbud MV. Disc in flames: roles of TNF-α and IL-1β in intervertebral disc degeneration. Eur Cell Mater 2015;30: 104–16. discussion 116-7. [eng].

[15] Wang Yongjie, Che Mingxue, Xin Jingguo, Zheng Zhi, Li Jiangbi, Zhang Shaokun. The role of IL-1β and TNF-α in intervertebral disc degeneration. Biomed Pharmacother 2020;131:110660 [eng].

[16] Andrade P, Visser-Vandewalle V, Philippens M, Daemen MA, Steinbusch HW, Buurman WA, et al. Tumor necrosis factor-alpha levels correlate with postoperative pain severity in lumbar disc hernia patients: opposite clinical effects between tumor necrosis factor receptor 1 and 2. Pain 2011;152(11):2645–52 [eng].

[17] Horii Manato, Orita Sumihisa, Nagata Maiko, Takaso Masashi, Yamauchi Kazuyo, Yamashita Masaomi, et al. Direct application of the tumor necrosis factor-α inhibitor, etanercept, into a punctured intervertebral disc decreases calcitonin gene-related peptide expression in rat dorsal root ganglion neurons. Spine (Phila Pa 1976) 2011;36:E80–5 [eng].

[18] Liu Weikun, Wang Yanfu. Protective role of the alpha-1-antitrypsin in intervertebral disc degeneration. J Orthop Surg Res 2021;16:516 [eng].

[19] Smolen JS, Weinblatt ME. When patients with rheumatoid arthritis fail tumour necrosis factor inhibitors: what is the next step? Ann Rheum Dis 2008;67(11): 1497–8 [eng].

[20] Aletaha D, Smolen JS. Diagnosis and management of rheumatoid arthritis: a review. Jama 2018;320(13):1360–72.

[21] Korhonen T, Karppinen J, Paimela L, Malmivaara A, Lindgren KA, Jarvinen S, et al. The treatment of disc herniation-induced sciatica with infliximab: results of a randomized, controlled, 3-month follow-up study. Spine (Phila Pa 1976) 2005; 30(24):2724–8 [eng].

[22] Genevay S, Viatte S, Finckh A, Zufferey P, Balague F, Gabay C. Adalimumab in severe and acute sciatica: a multicenter, randomized, double-blind, placebo-controlled trial. Arthritis Rheum 2010;62(8):2339–46 [eng].

[23] Genevay S, Finckh A, Zufferey P, Viatte S, Balague F, Gabay C. Adalimumab in acute sciatica reduces the long-term need for surgery: a 3-year follow-up of a randomised double-blind placebo-controlled trial. Ann Rheum Dis 2012;71(4):560–2 [eng].

[24] Freeman BJ, Ludbrook GL, Hall S, Cousins M, Mitchell B, Jaros M, et al. Randomized, double-blind, placebo-controlled, trial of transforaminal epidural etanercept for the treatment of symptomatic lumbar disc herniation. Spine (Phila Pa 1976) 2013;38(23):1986–94 [eng].

[25] Ohtori S, Miyagi M, Eguchi Y, Inoue G, Orita S, Ochiai N, et al. Epidural administration of spinal nerves with the tumor necrosis factor-alpha inhibitor, etanercept, compared with dexamethasone for treatment of sciatica in patients with lumbar spinal stenosis: a prospective randomized study. Spine (Phila Pa 1976) 2012;37(6):439–44 [eng].

[26] Cohen SP, Bogduk N, Dragovich A, Buckenmaier 3rd CC, Griffith S, Kurihara C, et al. Randomized, double-blind, placebo-controlled, dose-response, and preclinical safety study of transforaminal epidural etanercept for the treatment of sciatica. Anesthesiology 2009;110(5):1116–26 [eng].

[27] Tang W, Lu Y, Tian QY, Zhang Y, Guo FJ, Liu GY, et al. The growth factor progranulin binds to TNF receptors and is therapeutic against inflammatory arthritis in mice. Science 2011;332(6028):478–84 [eng].

[28] Blüml S, Binder NB, Niederreiter B, Polzer K, Hayer S, Tauber S, et al. Antiinflammatory effects of tumor necrosis factor on hematopoietic cells in a murine model of erosive arthritis. Arthritis Rheum 2010;62(6):1608–19.

[29] Pegoretti V, Baron W, Laman JD, Eisel ULM. Selective modulation of TNF–TNFRs signaling: insights for multiple sclerosis treatment. Front Immunol 2018;9(925) [English].

[30] McCoy MK, Tansey MG. TNF signaling inhibition in the CNS: implications for normal brain function and neurodegenerative disease. J Neuroinflammation 2008; 5:45. 45. [eng].

[31] Orti-Casan N, Wu Y, Naude PJW, De Deyn PP, Zuhorn IS, Eisel ULM. Targeting TNFR2 as a novel therapeutic strategy for alzheimer's disease. Front Neurosci 2019; 13:49 [eng].

[32] Zhao YP, Liu B, Tian QY, Wei JL, Richbourgh B, Liu CJ. Progranulin protects against osteoarthritis through interacting with TNF-alpha and beta-Catenin signalling. Ann Rheum Dis 2015;74(12):2244–53.

[33] Cui Y, Hettinghouse A, Liu C-j. Progranulin: a conductor of receptors orchestra, a chaperone of lysosomal enzymes and a therapeutic target for multiple diseases. Cytokine Growth Factor Rev 2019;45:53–64.

[34] Liu CJ. Progranulin: a promising therapeutic target for rheumatoid arthritis. FEBS Lett 2011;585(23):3675–80 [eng].

[35] Jian J, Li G, Hettinghouse A, Liu C, Progranulin. A key player in autoimmune diseases. Cytokine 2018;101:48–55 [eng].

[36] Jian J, Konopka J, Liu C. Insights into the role of progranulin in immunity, infection, and inflammation. J Leukoc Biol 2013;93(2):199–208 [eng].

[37] Liu C-j, Bosch X. Progranulin: a growth factor, a novel TNFR ligand and a drug target. Pharmacol Ther 2012;133(1):124–32 [eng].

[38] Bateman A, Bennett HP. The granulin gene family: from cancer to dementia. Bioessays 2009;31(11):1245–54 [eng].

[39] Hu Ming-Hsiao, Yang Kai-Chiang, Chen Yeong-Jang, Sun Yuan-Hui, Lin Feng-Huei, Yang Shu-Hua. Optimization of puncture injury to rat caudal disc for mimicking early degeneration of intervertebral disc. J Orthop Res 2018;36:202–11 [eng].

[40] Qian Jiale, Ge Jun, Qi Yan, Wu Cenhao, Yang Huilin, Zou Jun. Selection of the optimal puncture needle for induction of a rat intervertebral disc degeneration model. Pain Physician 2019;22:353–60 [eng].

[41] Driscoll T, Jacklyn G, Orchard J, Passmore E, Vos T, Freedman G, et al. The global burden of occupationally related low back pain: estimates from the Global Burden of Disease 2010 study. Ann Rheum Dis 2014;73(6):975–81 [eng].

[42] Liu H, Pan H, Yang H, Wang J, Zhang K, Li X, et al. LIM mineralization protein-1 suppresses TNF-alpha induced intervertebral disc degeneration by maintaining nucleus pulposus extracellular matrix production and inhibiting matrix metalloproteinases expression. J Orthop Res 2015;33(3):294–303 [eng].

[43] Sinclair SM, Shamji MF, Chen J, Jing L, Richardson WJ, Brown CR, et al. Attenuation of inflammatory events in human intervertebral disc cells with a tumor necrosis factor antagonist. Spine (Phila Pa 1976) 2011;36(15):1190–6 [eng].

[44] Gawri R, Rosenzweig DH, Krock E, Ouellet JA, Stone LS, Quinn TM, et al. High mechanical strain of primary intervertebral disc cells promotes secretion of inflammatory factors associated with disc degeneration and pain. Arthritis Res Ther 2014;16(1):R21 [eng].

[45] Hoyland JA, Le Maitre C, Freemont AJ. Investigation of the role of IL-1 and TNF in matrix degradation in the intervertebral disc. Rheumatology 2008;47(6):809–14 [eng].

[46] Zhang J, Wang X, Liu H, Li Z, Chen F, Wang H, et al. TNF-alpha enhances apoptosis by promoting chop expression in nucleus pulposus cells: role of the MAPK and NF-kappaB pathways. J Orthop Res 2019;37(3):697–705 [eng].

[47] Zhang Yuanqiang, Zhao Yunpeng, Li Jingkun, Wang Shuaishuai, Liu Yi, Nie Lin, et al. Interleukin-9 promotes TNF-α and PGE2 release in human degenerated intervertebral disc tissues. Spine (Phila Pa 1976) 2016;41:1631–40 [eng].

[48] Kaiser J, Allaire B, Fein PM, Lu D, Jarraya M, Guermazi A, et al. Correspondence between bone mineral density and intervertebral disc degeneration across age and sex. Arch Osteoporos 2018;13(1):123 [eng].